Electromagnetic Interference Analysis of Cabinet for Wireless HART Communication

Jaeyul Choo*, Sang Yong Jeong, Hyung Tae Kim, Yeong Jin Yu, Hyun Shin Park, and Choong Heui Jeong
Korea Institute of Nuclear Safety, 62 Gwahak-ro, Yuseong-gu, Daejeon, 305-338, Korea
**Corresponding author: k728cjy@kins re.kr*

1. Introduction

Wireless communication that delivers information through various frequency bands has long been gaining popularity because it offers various advantages such as mobility and convenience for access to communication networks. A recent study investigated the possibility of utilizing the wireless communication in the nuclear power plants in South Korea [1]. Among the protocols of the wireless communication, the wireless HART communication using the carrier frequency of 2.4 GHz has attracted a lot of interest due to the convenient monitoring and measurement of the variables of nuclear power plants. However the application of the wireless communication to nuclear power plants poses an on-going challenge due to the unwanted electromagnetic interference (EMI) caused by wireless devices, which would cause the detrimental malfunctioning to adjacent equipment. Especially the EMI problem in the cabinet containing digital instrument and control (I&C) devices is crucial to safety functions and should thus be treated electromagnetically before the use of the wireless communication in nuclear power plants is approved.

The mode-matching method has been widely used in electromagnetic analysis due to the reduced computing time by the fast convergence in series solutions [2]–[5]. Inspired by this, we perform the electromagnetic scattering analyses of an open cabinet using the mode-matching method. The resulting information of the electric (*E*) and magnetic (*H*) fields enables us to estimate how much the digital I&C in the cabinet is influenced by the external electromagnetic source.

2. Mode-Matching Formulation

Fig. 1 illustrates a cross section of the open cabinet that includes digital I&C devices at the center. We assume that the metallic cabinet is infinitely long along the *y*-axis and buried into infinite ground. We herein consider the incident and scattered electric fields are parallel to the *y*-axis (transverse electric (TE) field). The analyzed regions around the cabinet are composed of 6 regions (Regions I to VI) where we set 10 points from P_1 to P_{10} as our measurement points. In Region I, the electric field of the incident and the reflected plane waves are represented as

$$E_y^i = e^{i(k_x x - k_z z)} \tag{1}$$

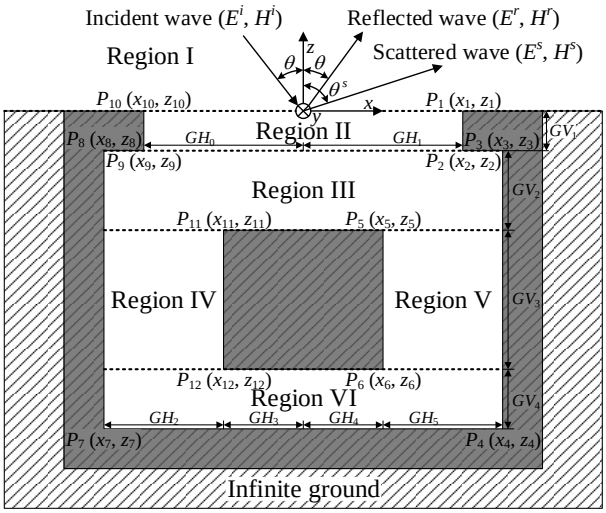

Fig. 1. Cross section of an open cabinet.

$$E_y^r = -e^{i(k_x x + k_z z)} \tag{2}$$

where $k_x = k_0 \sin\theta$, $k_z = k_0 \cos\theta$, and k_0 ($= \omega\sqrt{\mu_0 \varepsilon_0}$) is the wave number in free space. The electric fields in each region satisfy Helmholtz's equation as

$$(\nabla^2 + k_0^2)E = 0 \tag{3}$$

Based on the separation of variables and the Fourier transform, the solutions of (3) for each region are obtained as

$$E_y^s = \frac{1}{2\pi}\int_{-\infty}^{\infty} E_y^s(\zeta) e^{i(\kappa_0 z - \zeta x)} d\zeta \tag{4}$$

$$E_y^{II} = \sum_{m_2=1}^{\infty} \sin a_{m_2}(x - x_{10})(A_{m_2} \sin b_{m_2} z + B_{m_2} \cos b_{m_2} z) \tag{5}$$

$$E_y^{III} = \sum_{m_3=1}^{\infty} \sin a_{m_3}(x - x_8)(A_{m_3} \sin b_{m_3} z + B_{m_3} \cos b_{m_3} z) \tag{6}$$

$$E_y^{IV} = \sum_{m_4=1}^{\infty} \sin a_{m_4}(x - x_7)(A_{m_4} \sin b_{m_4} z + B_{m_4} \cos b_{m_4} z) \tag{7}$$

$$E_y^{V} = \sum_{m_5=1}^{\infty} \sin a_{m_5}(x - x_5)(A_{m_5} \sin b_{m_5} z + B_{m_5} \cos b_{m_5} z) \tag{8}$$

$$E_y^{VI} = \sum_{m_6=1}^{\infty} A_{m_6} \sin a_{m_6}(x - x_7) \sin b_{m_6}(z - z_7) \tag{9}$$

where $a_{m_2} = m_2\pi/(x_1 - x_{10})$, $a_{m_3} = m_3\pi/(x_3 - x_8)$, $a_{m_4} = m_4\pi/(x_{11} - x_7)$, $a_{m_5} = m_5\pi(x_4 - x_6)$, $a_{m_6} = m_6\pi/(x_4 - x_7)$, $b_{m_2} = \sqrt{k_0^2 - a_{m_2}^2}$, $b_{m_3} = \sqrt{k_0^2 - a_{m_3}^2}$, $b_{m_4} = \sqrt{k_0^2 - a_{m_4}^2}$, $b_{m_5} = \sqrt{k_0^2 - a_{m_5}^2}$, $b_{m_6} = \sqrt{k_0^2 - a_{m_6}^2}$, $\kappa_0 = \sqrt{k_0^2 - \zeta^2}$, and the superscription indicates each region in (5)–(9). In addition, the magnetic fields for each region can be obtained by

$$\nabla \times \bar{E} = i\omega\mu\bar{H} \tag{10}$$

To determine the unknown modal coefficients A_2, A_3, A_4, A_5, A_6, B_2, B_3, B_4, and B_5, the boundary conditions on tangential E- and H-field continuities should be applied. The E_y-continuity at $z = z_1 = 0$ is expressed as

$$E_y^i\Big|_{z=z_1} + E_y^r\Big|_{z=z_1} + E_y^s\Big|_{z=z_1} = \begin{cases} E_y^{II}\Big|_{z=z_1} & , \quad x_{10} < x < x_1 \\ 0 & , \quad \text{otherwise.} \end{cases} \tag{11}$$

Then applying the inverse Fourier transform to (11) yields

$$E_y^s = -\sum_{m_2=1}^{\infty} B_{m_2} a_{m_2} e^{i\zeta x_{10}} G(m_2, \zeta, \alpha) \tag{12}$$

where $G(m, \zeta, \alpha) = (-1)^m e^{i\zeta\alpha} - 1) / ((m\pi/\alpha)^2 - \zeta^2)$. Next, the H_x-continuity at $(x_{10} < x < x_1, z = z_1)$ is

$$H_x^i\Big|_{z=z_1} + H_x^r\Big|_{z=z_1} + H_x^s\Big|_{z=z_1} = H_x^{II}\Big|_{z=z_1} \tag{13}$$

Multiplying (13) by $\sin a_{p_2}(x - x_{10})$ and integrating the result with respect to x from x_{10} to x_1, we obtain

$$\begin{aligned} & 2k_z a_{p_2} e^{ik_x x_{10}} (x_6 - x_1) G(p_2, k_x, \alpha) \\ & = \sum_{m_2=1}^{\infty} ib_{m_2} A_{m_2} (x_1 - x_{10}) \delta_{m_2 p_2} \\ & + \sum_{m_2=1}^{\infty} B_{m_2} \left(\int_{-\infty}^{\infty} \frac{\kappa_0 a_{m_2} a_{p_2}}{\pi} G(m_2, \zeta, \alpha) G(p_2, -\zeta, \alpha) d\zeta \right). \end{aligned} \tag{14}$$

Note that the integral of the oscillatory function in (14) could be conveniently evaluated by the residue theorem [2]–[5]. Similarly, E_y- and H_x-continuities at z_3, z_5, and z_6 yield 8 equations. The obtained equations constitute the set of simultaneous equations for calculating the modal coefficients. The modal coefficients are obtained after truncating the infinite series in the simultaneous equations efficiently.

3. Computed Results

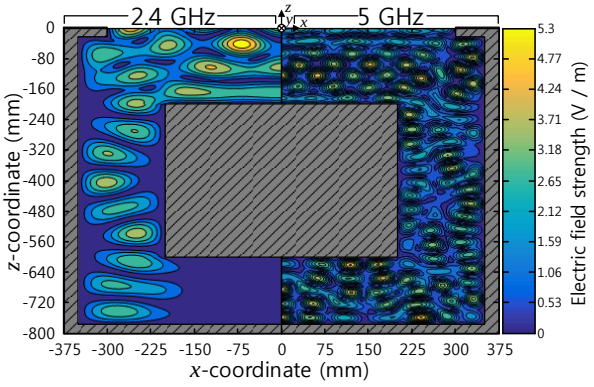

Fig. 2. Distribution of the electric field strength in the open cabinet.

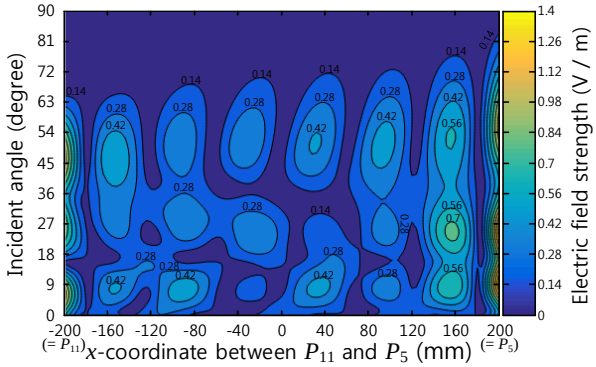

Fig. 3. Variation in the electric field strength on the surface between P_{11} and P_5 when the incident angle changes from 0° to 90°.

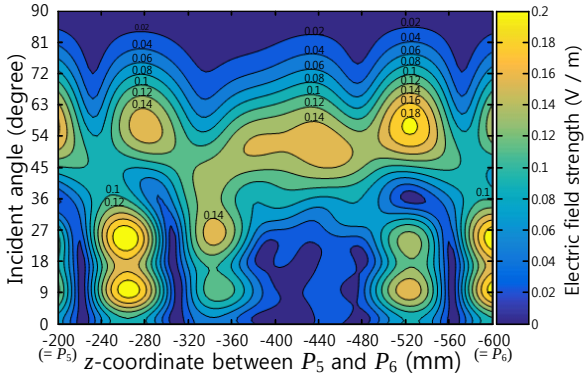

Fig. 4. Variation in the electric field strength on the surface between P_5 and P_6 when the incident angle changes from 0° to 90°.

Computation was performed to examine the electric field strength of the open cabinet whose geometrical parameters were set as $GH_0 = GH_1 = 300$ mm, $GH_2 = GH_5 = 150$ mm, $GH_3 = GH_4 = 200$ mm, $GV_1 = 25$ mm, $GV_2 = GV_4 = 175$ mm, and $GV_3 = 400$ mm. To check

the convergence of our series solutions, we investigated the absolute values of A_{m_2} , B_{m_2}, and $A_{m_2} \sin b_{m_2} z_\alpha + B_{m_2} \cos b_{m_2} z_\alpha$ when m_2 increases up to 9, the frequency is set to 5 GHz, and $z_\alpha = -GV_1 / 2$. The resulted variables showed that the infinite series converge quite rapidly, resulting in efficiency in numerical computation. Similarly, the convergence behavior of the infinite series in terms of other modal coefficients has also been confirmed. Fig. 2 shows the computed electric field distribution at 2.4 GHz and 5 GHz for wireless HART and 802.11 protocols when the TE plane wave in Region I has the incident angle of 0°. Due to the symmetric field distribution respect to the *y*–*z* plane, half of the resulting distribution for each frequency is represented. While the maximum field strength at 2.4 GHz is shown to be 3.48 V / m near the entrance of the cabinet ($x = \pm 70$ mm, $z = -40$ mm), that at 5 GHz is shown to be 5.36 V / m near the rear wall of the cabinet ($x = \pm 240$ mm, $z = -760$ mm). This result reveals that the EMI problem may become significant as the frequency of the external electromagnetic source increases.

To evaluate the effect due to the variation in an incident angle, we investigated the electric field strength at 2.4 GHz in the distance of 0.01 λ from the surface of the centered conductor. Figs. 3 and 4 show the variation in the electric field strength on the surface from P_{11} to P_5 and from P_5 to P_6, respectively, when the incident angle changes from 0° to 90°. Both results show the field strength drastically changes at the edge of the centered conductor (at P_5, P_6, and P_{11}). Especially the field strengths at $x = 160$ mm in Fig. 3 and at $z = -260$ mm in Fig. 4 change significantly due to the variation of the incident angle. In Fig 4, when the incident angle is around 55°, the electric field penetrates into the inside of the cabinet. The analysis performed in Figs. 3 and 4 can give a clue about the best placement for the digital I&C as well as the precaution against the external electromagnetic source in order to avoid the potential EMI problems.

4. Conclusion

The mode-matching method was applied to the scattering analysis of the open cabinet for the digital I&C in nuclear power plants. The mathematical expressions with the unknown modal coefficients for electromagnetic field distributions were formulated based on Helmholtz's equation in conjunction with both the separation of variables and the Fourier transforms. We then determined the modal coefficients from the boundary conditions for electric and magnetic field continuities. Using the obtained modal coefficients, the distribution and the variation of the electric field strength were investigated while varying the frequency and the incident angle of the TE incident plane wave. The investigated results provide us with the useful information to avoid EMI problems in the cabinet.

5. Acknowledgments

This work was supported by the Korea Institute of Nuclear Safety under the project 'Development of Proof Test Model and Safety Evaluation Techniques for the Regulation of Digital I&C Systems used in NPPs' (no. 1305003−0315−SB130).

REFERENCES

[1] D. Y. Ko and S. I. Lee, Applicable Approach of the Wireless Technology for Korean Nuclear Power Plants," Nuclear Engineering and Design, Vol. 265, pp. 519-525, Dec. 2013.
[2] H. J. Eom, Wave Scattering Theory, Springer Verlag, Berlin, 2001.
[3] H. H. Park and H. J. Eom, Electromagnetic Penetration into 2-D Multiple Slotted Rectangular Cavity: TM-Wave, IEEE Transaction on Antennas and Propagation, Vol. 48, No. 2, Feb. 2000.
[4] H. H. Park and H. J. Eom, Electromagnetic Penetration into a Rectangular Cavity with Multiple Rectangular Apertures in a Conducting Plane," IEEE Transaction on Electromagnetic Compatibility, Vol. 42, No. 3, Aug. 2000.
[5] T. J. Park and H. J. Eom, Scattering and Reception by a Flanged Parallel-Plate Waveguide: TE-Mode analysis, IEEE Transaction on Microwave Theory and Techniques, Vol. 41, No. 8, pp. 1458−1460, Aug. 1993.